

# Grow and multiply: the structure of turbulent energy cascades

Juan Luis Cabrera Fernández,<sup>1,2,3,\*</sup> Esther D. Gutiérrez,<sup>4,2,3</sup>

Miguel Rodríguez Márquez,<sup>5,3</sup> and Juan S. Medina-Alvarez<sup>3</sup>

<sup>1</sup>*Departamento de Física Aplicada, ETSI Aeronáutica y del Espacio,  
Universidad Politécnica de Madrid,*

*Pza. Cardenal Cisneros 3, 28040, Madrid, Spain*

<sup>2</sup>*Laboratorio de Dinámica Estocástica, Centro de Física,*

*Instituto Venezolano de Investigaciones Científicas, Caracas 1020-A, Venezuela*

<sup>3</sup>*Deeptikus Ltd., 10A Tasman Ave.,*

*Mount Albert, Auckland 1025, New Zealand*

<sup>4</sup>*Facultad de Ciencias Naturales y Matemáticas,*

*Escuela Superior Politécnica del Litoral,*

*Km 30.5 Vía Perimetral, Guayaquil, Ecuador*

<sup>5</sup>*Department of Biochemistry & Molecular Biology University of Calgary, T2N 4N1 Canada*

(Dated: May 26, 2022)

## Abstract

Neither from theoretical nor experimental approaches are fully developed turbulent flows really understood. In this dynamical state, the energy cascades from larger to smaller scales following a power law. However, there is still no detailed picture of the process that underlies such cascades. Here we show a mechanism to generate the analytical structure of a cascade from which the energy scaling law for isotropic homogeneous turbulence emerges. We deduce a function that unveils a non self-similar multifractal as the cascade's origin. This insight reveals that the backbone underlying cascades is formed by deterministic nested polynomials. The obtained cascade behaves as expected for turbulent flows in the presence of fluctuations and fulfills the Onsager's conjecture. This work shows that turbulent cascade behavior is obtainable from simple nonlinear dynamics.

Keywords: Turbulence, fractals, nonlinear maps

Despite the efforts done to understand turbulence it still remains an open problem. Much of the advances in this area have been inspired by Richardson's [1] cascade idea, which was later developed by Kolmogorov [2] and Onsager [3]. However, we don't have a detailed analytical description of energy cascades. If we had such a description we would be able to gain a deeper insight into the inner workings of turbulence. It would impact positively the development of a theory of turbulence and related technologies. An increase in our understanding on turbulence must result in the development of important practical applications, including flow resistance reduction which would translate into global savings in energy consumption [4]. This work details how a cascade is analytically structured.

In Richardson's picture nonlinearity transforms large-scale velocity circulations (eddies) into circulations at successively smaller scales until reaching a small scale where eddies are dissipated by viscosity. Over time, there has been important advances in our understanding of the physics involved in this picture, as the notion of inertial range [2], the derivation of the  $-5/3$  power law energy spectrum either analytically [2, 5–8] or by numerical simulation of shell models [9], the verification of lack of self-similarity [10], the experimental corroboration that energy dissipation is independent of the molecular viscosity [11] or the velocities's non-Gaussian distribution and strong acceleration intermittency [12].

From these aspects it is worth noting that intermittency is not an exclusive behavior of turbulent flows. It can be found in many complex systems [13–21]. So what do intermittent systems have to say about turbulent cascades? To address this question, we analyze a low dimensional multiplicative dynamics able to display intermittency. Consider the following map (See Supplemental Material sections 1 – 7 for mathematical details)

$$x_{g+1} = r_g x_g (1 - x_{g-1}), \quad (1)$$

where  $g = 1, \dots, +\infty$ , is an iteration index,  $r_g : r(g)_{a,b}$ , is some random perturbation indexed by  $g$ , of intensity  $a$ , and bias  $b$ . We linearize (1) around the fixed point  $\alpha \equiv 1 - \frac{1}{\beta}$  to obtain,

$$| X_{g+1} \rangle = \mathbf{A}_g | X_g \rangle + | B_g \rangle, \quad (2)$$

written in terms of the vector  $| X_g \rangle \equiv \begin{pmatrix} x \\ y \end{pmatrix}_g$ , the evolution matrix  $\mathbf{A}_g \equiv \begin{pmatrix} r_g/\beta & -\alpha r_g \\ 1 & 0 \end{pmatrix}$  and a bias vector  $B_g \equiv \begin{pmatrix} \alpha^2 r_g \\ 0 \end{pmatrix}$ . Here,  $y_g \equiv x_{g-1}$ ,  $\beta$  is the mean value of  $r_g$ . Eq. (2) can be

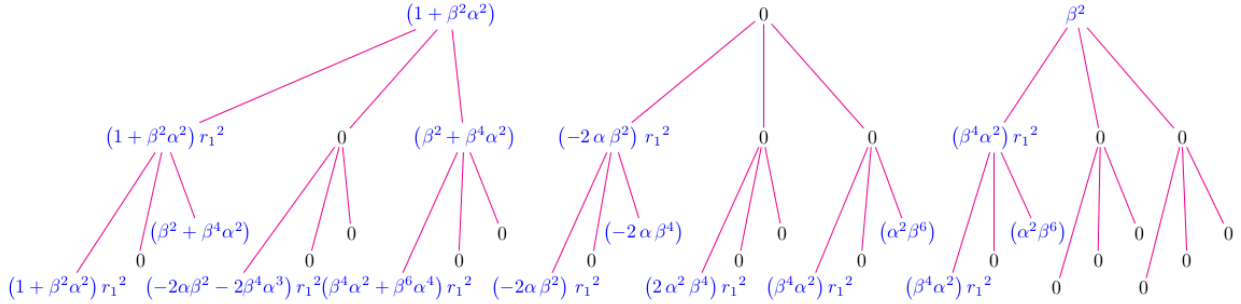


FIG. 1. Tree representation for the generation of the polynomial coefficients after two iterations of rule (4), starting from  $\Lambda_1$ . Bottom coefficients are those forming  $\Lambda_3$  given by Eq. (3).

expanded to obtain,  $|X_g\rangle = \mathbf{P}_g |X_0\rangle + \sum_{i=1}^g \mathbf{P}_i |B_{i-1}\rangle$ , which simplifies as,  $|X_g\rangle = \gamma_g \mathbf{P}_g |X_0\rangle$ , where  $\gamma$  is an unbounded random variable larger than 1, i.e., it has an applying effect on  $\mathbf{P}_g$ . This expression is written in terms of the matrix product  $\mathbf{P}_g \equiv \prod_{j=0}^{g-1} \mathbf{A}_j$ . To calculate the norm of  $|X_g\rangle$  we must calculate  $\mathbf{P}_g^\dagger \mathbf{P}_g = \mathbf{A}_0^\dagger [\mathbf{A}_1^\dagger \dots [\mathbf{A}_{g-2}^\dagger [\mathbf{A}_{g-1}^\dagger \mathbf{A}_{g-1}] \mathbf{A}_{g-2}] \dots \mathbf{A}_1] \mathbf{A}_0$ , with  $\mathbf{A}_g^\dagger = \begin{pmatrix} r_g/\beta & 1 \\ -r_g\alpha & 0 \end{pmatrix}$ , the adjoint matrix. We solved the eigenvalue problem iteratively starting from the first inverse one,  $\mathbf{A}_0^\dagger = \mathbf{A}_0^{-1}$ , which gives  $\lambda_0^{p_1} = 1 / \left( \lambda_0 + \sqrt{\lambda_0^2 - \gamma^2} \right)$ .

starting from the first inner one,  $p_1 \equiv \mathbf{A}_{g-1}^T \mathbf{A}_{g-1}$ , which gives,  $\lambda_{\pm}^{p_1} = \frac{1}{2\beta^2} \left( \Lambda_1 \pm \sqrt{\Lambda_1^2 - \Upsilon_1^2} \right)$ , with  $\Lambda_1 \equiv (1 + \beta^2 \alpha^2) r_1^2 + \beta^2$  and  $\Upsilon_1 \equiv 2\beta^2 \alpha r_1$ . The calculation of higher order products allowed us to obtain  $\lambda_{\pm}^{p_g} = \frac{1}{2\beta^{2g}} \left( \Lambda_g \pm \sqrt{\Lambda_g^2 - \Upsilon_g^2} \right)$  and from it to deduce the leading term  $\Lambda$ . We can grasp how these eigenvalues behave by observing the way the term  $\Lambda_3$  is assembled,

$$\Lambda_3 \equiv \left\{ \begin{array}{l} \left[ (1 + \beta^2 \alpha^2) r_1^2 \right] r_2^2 \\ + \left[ (\beta^2 + \beta^4 \alpha^2) \right] r_2 \\ + \left[ (-2 \alpha \beta^2 - 2 \beta^4 \alpha^3) r_1^2 \right] r_2 \\ + \left[ (\beta^4 \alpha^2 + \beta^6 \alpha^4) r_1^2 \right] \end{array} \right\} r_3^2 \quad (3)$$

The eigenvalues for larger  $g$ 's are nested order two polynomials in the noise terms  $r_g, r_{g-1}, \dots, r_1$  (See Supplemental Material at sections 8 – 10 for larger  $\Lambda_g$ 's). In gen-

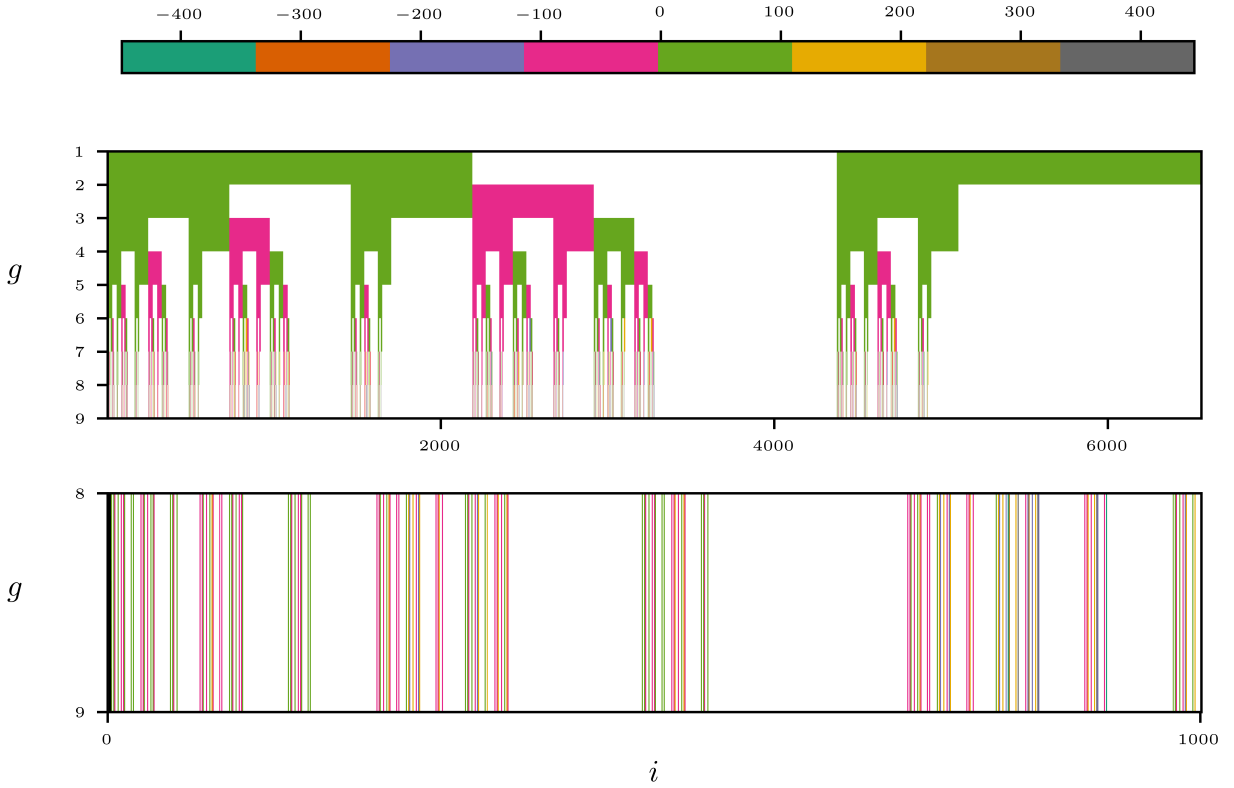


FIG. 2. (Top) Analytical deterministic cascade describing the evolution of the nested polynomial coefficients  $C_2$ ,  $C_1$  and  $C_0$  (from left to right) after  $n = 8$  iterations. Colors represent the coefficient's intensities  $a_i$ . The iteration process starts with the  $\Lambda_1$  coefficients, each one laying on  $\frac{1}{3}$  segments on the  $x$ -axis which hosts  $3^8$  subdivisions. (Bottom) Zoom in the interval  $[0, 1000]$  showing fine structure. Parameter values are  $r = 1$ ,  $a = 0.085$  and  $b = 1.9375$ .

eral, if we know  $\Lambda_1$  and  $\Lambda_2$ , we can obtain  $\Lambda_g$  given that, in the generation  $g - 1$ , the term  $\{C_2 r_i^2 + C_1 r_i + C_0\} r_{i+1}^k$ , with  $k = 0, 1, 2$ ; generates the polynomial

$$\left\{ \begin{array}{l} [C_2 r_i^2 + C_1 \chi_1 r_i + \beta^2 C_2] r_{i+1}^2 \\ + [-k\alpha\beta^2 C_2 r_i^2 + C_1 \chi_2 r_i + C_1 \chi_3] r_{i+1} \\ + [\beta^2 \alpha^2 C_0 r_i^2 + C_1 \chi_4 r_i + C_1 \chi_5] \end{array} \right\} r_{i+2}^k, \quad (4)$$

in the next generation  $g$ . There is no need to determine the unknowns,  $\chi_1, \chi_2, \dots, \chi_5$ , because in the current situation  $C_1 = 0$  (See Supplemental Material at section 10 for an example obtaining  $\Lambda_3$  from  $\Lambda_2$ ).

The hidden structure of the  $\Lambda_g$ 's is better realized in a graphical representation. Figure 1 shows the branching process obtained after just three iterations of the rule (4). The terms

displayed at the bottom form  $\Lambda_3$  (See Supplemental Material at sections 8 for additional detail). The figure reveals an analytical cascading process that dictates the eigenvalues's inner mathematical backbone. To analyze this deterministic backbone we turn off randomness by setting  $r_g = 1, \forall g$ . Also, we select  $a + b$  such that the system is near a Hopf bifurcation. A temporal window displaying the cascade obtained with these conditions is depicted in figure 2. The coefficient values in the initial polynomial  $\Lambda_1$ , i.e.,  $C_2$ ,  $C_1$  and  $C_0$ , define the intensity on the unit interval subsets,  $I_2 \equiv [0, \frac{1}{3}]$ ,  $I_1 \equiv [\frac{1}{3}, \frac{2}{3}]$  and  $I_0 \equiv [\frac{2}{3}, 1]$ , respectively. After one iteration, each subset is divided by a factor of 3 and the new generated coefficients update the intensity in the new  $N_2 = 3^2$  subintervals. After each new generation, the unit interval is divided by a factor of 3 such that, after  $g$  iterations the coefficients lay on  $N_g = 3^g$  subintervals, each one displaying its own intensity given by (4). In figure 2 we can see how fast the analytical cascade grows: after  $g = 8$  the unit subinterval harbors  $N_8 \sim 3^8 = 6561$  coefficients in the same number of subintervals. Because  $r_g = 1, \forall g$ , this fractal analytical cascade is the support on which non zero random perturbations will affect the norm or any other quantity calculated from it. The bottom part of figure 2 shows a detail of the fine structure of this geometrical object.

The obtained structure is not self-similar:  $I_2$  is the only segment obeying a self-similar rule, which is given by,  $X_{g+1} = \frac{X_g}{3}; X \in I = [0, 1]$ . Subintervals  $I_1$  and  $I_0$  does not seem to follow a self-similar rule. The mapping process shows an independent progression for each of the initial  $I_i$  intervals, yielding a non self-similar structure with multifractal characteristics. A full characterization of this object will be carried out elsewhere. Branch intensities,  $a_i$ ,  $i = 1 \dots 3^g$ , display a non trivial behavior as seen in figure 3. We plotted  $a_i$  for each branch on the limit set after  $g = 15$  iterations. The horizontal axis contains  $N_{15} = 3^{15} = 14.348.907$  points. Successive enlargements of the initial interval shows statistically equivalent objects as expected for a fractal. The figure also shows that the lack of self-similarity extends to both, the branch positions and their intensities. The behavior of the distribution of intensities (figure 5) is comparable with Thomae's self-similar function as has been reported also for high-throughput biological and clinical data [22].

At this point let's consider the following: 1) In turbulence the energy cascades through length scales, 2) in the cascade described by (4) each scale is given by a generation level, 3) therefore, in the analytical cascade length scale changes are captured by changes in  $g$ , 4) because differential operators in real space transform into multiplicative operators

in the  $k$ -space, the diffusion operator in the Navier-Stokes (NS) equation becomes a  $k^2$  term in a Fourier representation and 5) the essential interactions in turbulence cascades are between wave numbers of similar magnitude [3, 23]. On these grounds, let's conjecture that the quadratic nonlinearity in (1) describes the interaction between a cascade level characterized by some function of the wavenumber,  $f(k_g)$ , and a vicinity level of similar magnitude characterized by the function,  $f(k_{g-1})$ . To this conjecture we add the following ansatz:  $E(k) \sim E(g) \equiv f(k)$ . Hence, an evaluation of the energy cascading down with each change in scale must consider all the non-zero  $k$  contributions. So, let's say that, if at a fixed cascading scale  $g$ ,  $a_k$  is the intensity of an individual branch representing a wavenumber  $k$ , and there are  $l_g$  non-zero intensities then, the total energy at that length scale is the mean value of the  $a_k$ 's, i.e.,

$$E(k) \sim E(g) \equiv \sum_{\forall a_k \neq 0} \frac{a_k(g)}{l_g}. \quad (5)$$

This expression informs about the mean energy contained on the full set of  $l_g$  branches at a fixed generation step  $g$  as untangled by the recurrence (4). The values of  $E(k) \sim E(g)$  calculated for the analytical cascade are circles in figure 4(Top). These results are compared with a solid line that follows a power law with the Kolmogorov's exponent  $-5/3$  [2]. They follow the trend expected for the energy spectrum in fully developed isotropic homogeneous turbulence [24], i.e., it is shown that,  $E(k) \sim E(g) = g^{-5/3}$ . The range of generation values may seem small,  $g = 19$ . However, the number of branches are not, it is  $l_{19} = 3.759.853$ . With our current computer power we limited the calculations to  $g = 19$  generations.

We expect departures from the power law when turning the noise on. When (4) is recreated in the simplest noisy case with  $a = 1$  and  $b = 0$  and  $E(k) \sim E(g)$  measured with Eq. (5), calculated points initially close to the power law deviate notoriously from it as the cascade level increases. Thus, the analytical cascade with active noise behaves the same as turbulence energy cascades. It indicates that the dynamics described by (4) captures the dissipation of energy produced by random fluctuations as measured by Eq. (5). It follows that, in the noise free situation, the analytical cascades would continue without end, meaning that increasing  $g$  to much larger values shall still follow the  $-5/3$  law, i.e., extending the inertial range to infinity. This is a result in the line with the Onsager's conjecture that dissipation energy might exist even in the limit of vanishing viscosity [3, 6].

While these results may seem encouraging, the limited power law range is disappointing.

Consequently, we explore additional possibilities for the ansatz  $E(k) \sim E(g) \equiv f(k)$ . In particular, we consider,

$$E(k) \sim E(g) \equiv \sum_{\forall a_k \neq 0} |a_k(\frac{1}{l_n(g)})|. \quad (6)$$

When this measure is applied to the deterministic case circles as those shown in figure 4(Bottom) are obtained. It can be seen that the curve follows a  $-5/3$  power law covering six orders of magnitude. The accuracy of such a result is remarkable and it seems to suggest that a better length scale estimation is given by  $\frac{1}{l_g}$ . When the calculation with the noise turned on ( $a = 1$  and  $b = 0$ ) is carried out the results deviate from a decreasing trend as one may initially expect (see figure 4(Bottom)). However, this result is pointing out some interesting aspects of the cascading process. A first one is that the behavior of the deterministic cases, as measured by Eq. (5) and Eq. (6), put emphasis on the deterministic origin of the  $-5/3$  power law: the energy scaling is independent of how we calculate it, by using the plain  $a$ 's or

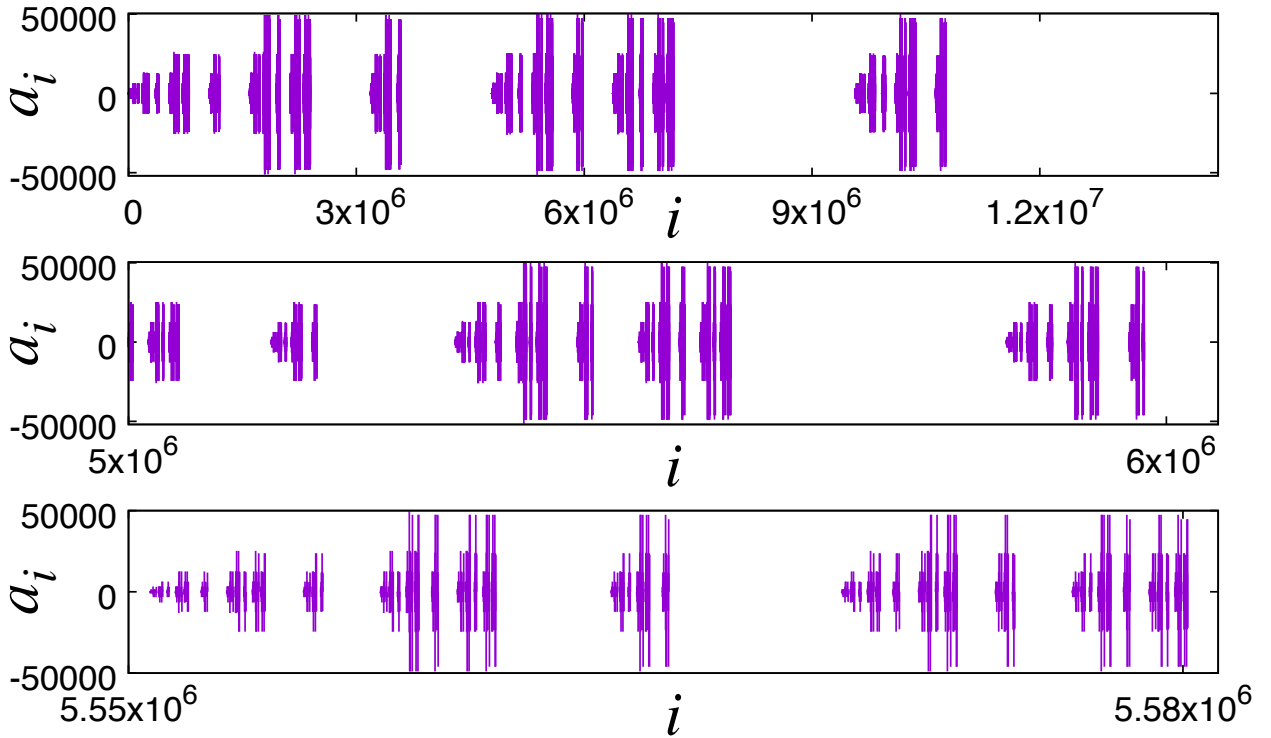


FIG. 3. Non self-similar structure of the analytical deterministic cascade revealed after successive enlargements. Image obtained with  $g = 15$  generations and parameter values as in Fig 2. The number of coefficients calculated is  $3^{15} = 14.348.907$ . Points are represented by impulses and zero ones have been extracted.

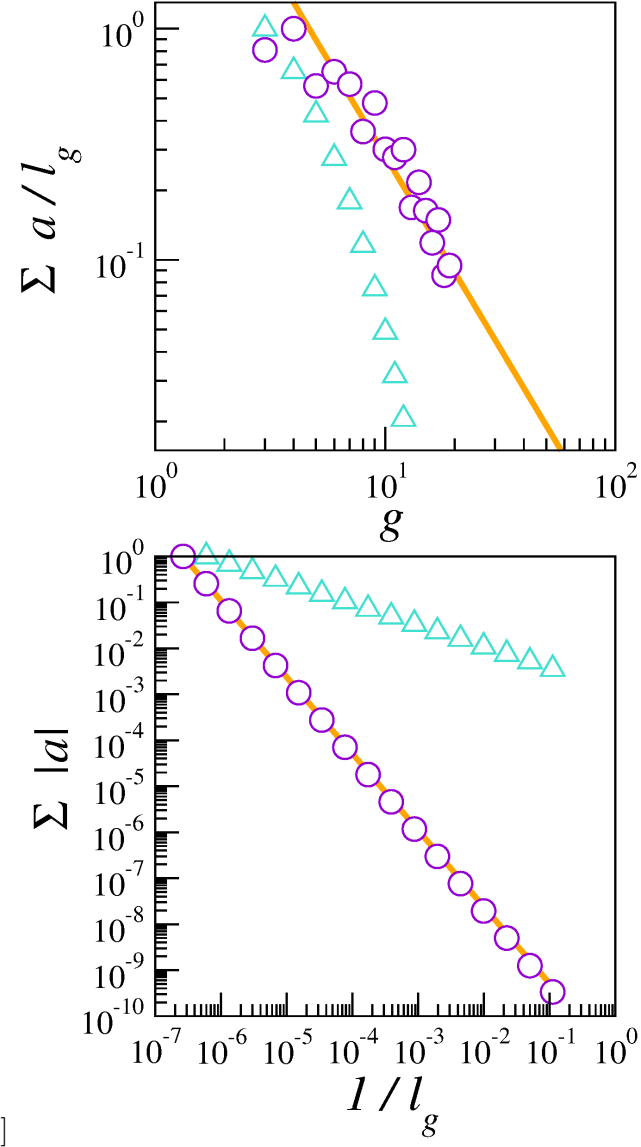


FIG. 4. (Top) Normalized results for  $\sum \frac{a}{l}$  as a function of the cascade level. Circles: points obtained for the deterministic backbone obtained with the same parameter values as in Fig 2. Triangles: results obtained in the simplest noisy situation with  $a = 1$  and  $b = 0$ . (Bottom) Normalized results for  $\sum |a|$  as a function of  $\frac{1}{l}$  in the same cases as in (Top). In both situations the straight line is a  $-\frac{5}{3}$  power law.

their norms. It means that the power law is rooted in the fractal structure of the cascading process's deterministic backbone. The situation turns out different when the noise is on. In such a case the fluctuation's intensities add on as measured by the norm present in Eq. (6) but cancel themselves in Eq. (5). Thus, Eq. (6) may be conserving the energy injected

into the cascade by randomness while Eq. (5) could be a better measure of its relative importance, probably more related to a proper calculation of a power spectrum. These last points deserve additional consideration in future research.

The obtainment of the  $-5/3$  exponent strongly suggests that turbulence energy cascades are ruled by an analytical structure equal, or at least similar, as the one discovered here. In such a case, the quadratic nonlinearity in Eq. (1) would be capturing the intersecting dynamics of the NS trajectories with a lower dimensional Poincare section. Then, Eq. (4) could be useful to bridge the higher dimensional trajectories of the NS solutions and the lower dimensional dynamics of Eq. (1). This research also suggest that the NS diffusion operator is the main actor in such intersections and no further term seem to be involved in the generation of the energy cascade.

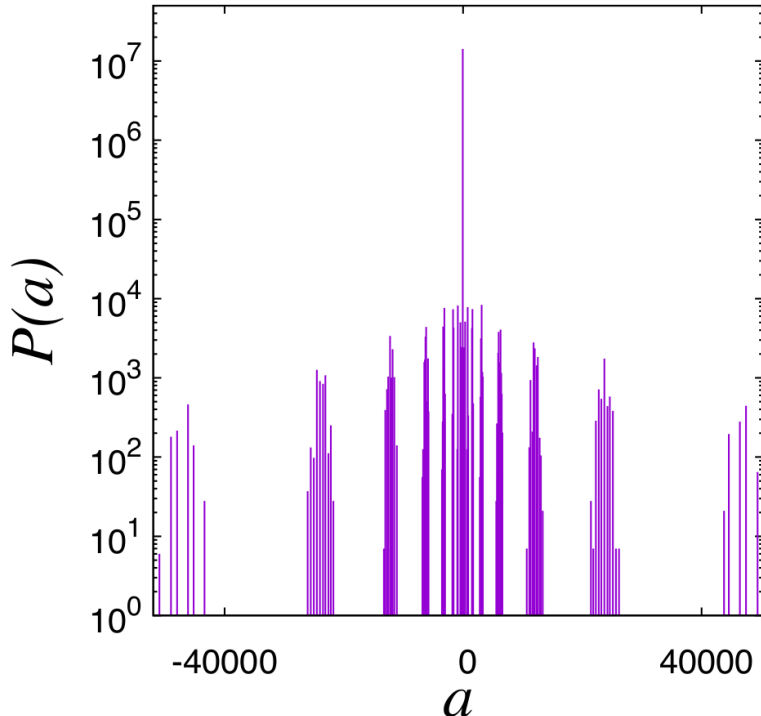


FIG. 5. Semi-log plot of the intensity distribution from the deterministic cascade obtained after 15 generations. Same parameter values as in figure 2.

Historically, low dimensional dynamical systems provided important insights into the onset of turbulence [25] and established a background on which improved understanding of turbulence has been achieved [10, 26, 27]. This work adds further evidence of the relevance of low dimensional discrete dynamics to understand turbulence. Furthermore, as intermittency

and non-Gaussian statistics can be observed in many complex systems [28, 29] it may also be the case for turbulent cascades, which may not be exclusive for fluids but a shared dynamical state rooted solely in nonlinear dynamics [26]. Our results provide support for that conception. We anticipate these results are a starting point for new analytical and numerical approaches of cascading phenomena, with the potential to impact a broad range of fields ranging from astrophysics to climatology and engineering.

JLCF acknowledges support from IVIC-141 grant during a small part of this work and from Prof. M. C. Pereyra (UNM). JLCF conceived, directed and developed all aspects of this research. MRM contributed with software development and simulation validations, EG and JMA independently validated the analytics. All authors contributed with paper writing.

## SUPPLEMENTARY MATERIAL FOR “GROW AND MULTIPLY: THE STRUCTURE OF TURBULENT ENERGY CASCADES”

### The DRM

A seemingly simple map that shows on-off intermittency is the random version of the delayed regulation model (DRM), which is given by the map on the unit interval,  $x \in [0, 1]$ ,

$$x_{g+1} = r_g x_g (1 - x_{g-1}), \quad (7)$$

with  $g = 1, \dots, +\infty$ , the iteration index,  $r_g : r(g)_{a,b}$ , is a random parametric perturbation indexed by  $g$  that depends on intensity,  $a$ , and bias,  $b$ , parameters. Our analysis is not restricted to a particular distribution of  $r_g$ , but for simplicity we may write it as,  $r_g = au_g + b$ . A simple case is considering  $u_g$  a uniformly distributed random variable in  $[0, 1]$ , so that  $r_g \in [b, a + b]$ . For the case of zero delay and noise, the map is the well known deterministic logistic map. Eq. (7) is probably one of the simplest dynamical models containing nonlinearities, time delay and parametric randomness. The deterministic counterpart of (7) has been widely studied [30–33] and its non-deterministic version has been useful to analyze stochastic extinction [34, 35], autonomous stochastic resonance [36] and noise-induced localization phenomena [37]. Eq. (7) shows sustained intermittency for parameter values  $a$  and  $b$  tuned at the boundaries displayed in the Figure 6. The first boundary corresponds to intermittency produced by the destabilization of the origin while the second boundary refers to intermittency produced by the destabilization of the fix point  $1 - 1/\langle r_g \rangle$ , which produces bursts involving limit cycle oscillations (the DRM undergoes a Hopf bifurcation at  $r_H = 2$ ). While the following analysis is carried out around the second boundary our results also apply for the fix point zero ( $\beta = 1$ ).

### Linealization of the DRM

The time delayed stochastic rule given by Eq. (1) can be rewritten as

$$x_{g+1} = r_g F(x_g, y_g) \quad (8)$$

$$y_{g+1} = G(x_g, y_g) \quad (9)$$

with  $F(x, y) = x(1 - y)$  and  $G(x, y) = x$ .  $F$  and  $G$  can be expanded around the fix point  $P \equiv (\alpha, \alpha)$  with  $\alpha \equiv 1 - 1/r_g = 1 - \frac{1}{\beta}$ , to obtain,

$$F(x, y) = F(\alpha, \alpha) + (x - \alpha) \frac{\partial F}{\partial x} \Big|_P + (y - \alpha) \frac{\partial F}{\partial y} \Big|_P + O(x^2, y^2) \quad (10)$$

$$G(x, y) = G(\alpha, \alpha) + (x - \alpha) \frac{\partial G}{\partial x} \Big|_P + (y - \alpha) \frac{\partial G}{\partial y} \Big|_P + O(x^2, y^2), \quad (11)$$

i.e.,

$$F(x, y) = \alpha^2 + (1 - \alpha)x - \alpha y \quad (12)$$

$$G(x, y) = x \quad (13)$$

Thus, near to the fix point  $P$  equation (1) can be approximated by its linear part,

$$x_{g+1} = r_g \left( \alpha^2 + \frac{x_g}{\beta} - \alpha y_g \right) \quad (14)$$

$$y_{g+1} = x_g. \quad (15)$$

And it can be rewritten as,

$$\begin{pmatrix} x \\ y \end{pmatrix}_{g+1} = \begin{pmatrix} r_g/\beta & -\alpha r_g \\ 1 & 0 \end{pmatrix} \begin{pmatrix} x \\ y \end{pmatrix}_g + \begin{pmatrix} \alpha^2 r_g \\ 0 \end{pmatrix}. \quad (16)$$

Now defining the evolution matrix,

$$\mathbf{A}_g \equiv \begin{pmatrix} r_g/\beta & -\alpha r_g \\ 1 & 0 \end{pmatrix} \quad (17)$$

and the bias vector,

$$B_g \equiv \begin{pmatrix} \alpha^2 r_g \\ 0 \end{pmatrix}, \quad (18)$$

Eq. 16 can be written in Dirac's bra-ket notation as,

$$|X_{g+1}\rangle = \mathbf{A}_g |X_g\rangle + |B_g\rangle \quad (19)$$

**Expanding  $|X_g\rangle$**

It is useful to express  $|X_g\rangle$  in terms of the initial state  $|X_0\rangle$ . Therefore, note that  $|X_{g+1}\rangle$  can be patiently developed as follows,

$$|X_{g+1}\rangle = \mathbf{A}_g |X_g\rangle + |B_g\rangle$$

$$\begin{aligned}
&= \mathbf{A}_g(\mathbf{A}_{g-1} | X_{g-1}\rangle + | B_{g-1}\rangle) + | B_g\rangle \\
&= \mathbf{A}_g(\mathbf{A}_{g-1}(\mathbf{A}_{g-2} | X_{g-2}\rangle + | B_{g-2}\rangle) + | B_{g-1}\rangle) + | B_g\rangle \\
&= \mathbf{A}_g(\mathbf{A}_{g-1}(\mathbf{A}_{g-2}(\mathbf{A}_{g-3} | X_{g-3}\rangle + | B_{g-3}\rangle) + | B_{g-2}\rangle) + | B_{g-1}\rangle) + | B_g\rangle \\
&= \mathbf{A}_g(\mathbf{A}_{g-1}(\mathbf{A}_{g-2}(\mathbf{A}_{g-3}(\dots\mathbf{A}_1(\mathbf{A}_0 | X_0\rangle + | B_0\rangle) \dots) + | B_{g-3}\rangle) + | B_{g-2}\rangle) + | B_{g-1}\rangle) + | B_g\rangle \\
&= \mathbf{A}_g \mathbf{A}_{g-1} \mathbf{A}_{g-2} \mathbf{A}_{g-3} \dots \mathbf{A}_1 \mathbf{A}_0 | X_0\rangle + \mathbf{A}_g \mathbf{A}_{g-1} \mathbf{A}_{g-2} \mathbf{A}_{g-3} \dots \mathbf{A}_1 | B_0\rangle + \dots + \\
&\quad + \mathbf{A}_g \mathbf{A}_{g-1} \mathbf{A}_{g-2} | B_{g-3}\rangle + \mathbf{A}_g \mathbf{A}_{g-1} | B_{g-2}\rangle + \mathbf{A}_g | B_{g-1}\rangle + | B_g\rangle
\end{aligned} \tag{20}$$

Then  $| X_{g+1}\rangle$  can be written as,

$$\begin{aligned}
| X_{g+1}\rangle &= \prod_{j=0}^g \mathbf{A}_{g-j} | X_0\rangle + \prod_{j=0}^{g-1} \mathbf{A}_{g-j} | B_0\rangle + \prod_{j=0}^{g-2} \mathbf{A}_{g-j} | B_1\rangle + \prod_{j=0}^{g-3} \mathbf{A}_{g-j} | B_2\rangle + \dots \\
&\quad + \prod_{j=0}^{g-(g-2+1)=1} \mathbf{A}_{g-j} | B_{g-2}\rangle + \prod_{j=0}^{g-(g-1+1)=0} \mathbf{A}_{g-j} | B_{g-1}\rangle + | B_g\rangle \\
&= \prod_{j=0}^g \mathbf{A}_{g-j} | X_0\rangle + \sum_{i=1}^{g+1} \prod_{j=0}^{g-i} \mathbf{A}_{g-j} | B_{i-1}\rangle.
\end{aligned} \tag{21}$$

Where we used the definition,

$$\prod_{j=0}^{g-i} \mathbf{A}_{g-j} \equiv 1 \text{ if } i = g+1. \tag{22}$$

Next, changing variables,  $g \rightarrow g' - 1$ , we obtain,

$$| X_g\rangle = \prod_{j=0}^{g-1} \mathbf{A}_{g-j-1} | X_0\rangle + \sum_{i=1}^g \prod_{j=0}^{g-i-1} \mathbf{A}_{g-j-1} | B_{i-1}\rangle, \tag{23}$$

where we have omitted the prime and used,

$$\prod_{j=0}^{g-i-1} \mathbf{A}_{g-j-1} \equiv \mathbf{1} \text{ if } i = g. \tag{24}$$

Thus, we can define,

$$\mathbf{P}_i \equiv \prod_{j=0}^{g-i-1} \mathbf{A}_{g-j-1} \quad \text{if } i \neq g, \tag{25}$$

$$\mathbf{P}_i \equiv \mathbf{1} \quad \text{if } i = g,$$

$$\mathbf{P}_g \equiv \prod_{j=0}^{g-1} \mathbf{A}_j, \tag{26}$$

to write  $| X_g\rangle$  in compact form,

$$| X_g\rangle = \mathbf{P}_g | X_0\rangle + \sum_{i=1}^g \mathbf{P}_i | B_{f(i)}\rangle, \tag{27}$$

with  $f(i) \equiv i - 1$ .

**Simplifying**  $| X_g \rangle = \mathbf{P}_g | X_0 \rangle + \sum_{i=1}^g \mathbf{P}_i | B_{f(i)} \rangle$

Let be  $| X'_g \rangle$  a state at generation  $g$  obtained with a realization  $r'_g \neq r_g$  and  $\langle X'_g |$  its complex conjugate. Applying this bra on the left of Eq. (12) we obtain,

$$\langle X'_g | X_g \rangle = \langle X'_g | \mathbf{P}_g | X_0 \rangle + \langle X'_g | \sum_{i=1}^g \mathbf{P}_i | B_{f(i)} \rangle. \quad (28)$$

The quantity  $\eta_g \equiv \langle X'_g | X_g \rangle$  is the coefficient for the projection of  $X_g$  onto  $X'_g$ . It is just a random variable evaluated at generation  $g$ . It takes values on the interval  $[0, 1]$ . Note also that applying the operator  $\mathbf{P}_g$  on the initial condition  $| X_0 \rangle$  produces a new state at generation  $g$ , say  $| \mu_g \rangle$ . Thus, applying the bra  $\langle X'_g |$  on  $\mathbf{P}_g | X_0 \rangle = | \mu_g \rangle$  yields also a random variable at generation  $g$ , say  $0 \leq \mu_g \leq 1$ , i.e.,

$$\langle X'_g | \mathbf{P}_g | X_0 \rangle = \langle X'_g | \mu_g \rangle \equiv \mu_g \quad (29)$$

With these considerations in mind we rewrite Eq. (28) as,

$$\begin{aligned} \eta_g &= \mu_g + \langle X'_g | \sum_{i=1}^g \mathbf{P}_i | B_{f(i)} \rangle \\ &= \mu_g \left( 1 + \mu_g^{-1} \langle X'_g | \sum_{i=1}^g \mathbf{P}_i | B_{f(i)} \rangle \right). \end{aligned} \quad (30)$$

After rearranging terms, it results in,

$$\mu_g \left( \frac{\eta_g}{\mu_g} - 1 \right) = \langle X'_g | \sum_{i=1}^g \mathbf{P}_i | B_{f(i)} \rangle \quad (31)$$

or

$$\langle X'_g | \mu_g \rangle \left( \frac{\eta_g}{\mu_g} - 1 \right) = \langle X'_g | \sum_{i=1}^g \mathbf{P}_i | B_{f(i)} \rangle, \quad (32)$$

where we have used (29). This expression is the same as,

$$\langle X'_g | \left( \frac{\eta_g}{\mu_g} - 1 \right) | \mu_g \rangle = \langle X'_g | \sum_{i=1}^g \mathbf{P}_i | B_{f(i)} \rangle, \quad (33)$$

from which it is clear that,

$$\left( \frac{\eta_g}{\mu_g} - 1 \right) | \mu_g \rangle = \sum_{i=1}^g \mathbf{P}_i | B_{f(i)} \rangle. \quad (34)$$

Now, using the definition of  $| \mu_g \rangle$ , it turns out that,

$$\left( \frac{\eta_g}{\mu_g} - 1 \right) \mathbf{P}_g | X_0 \rangle = \sum_{i=1}^g \mathbf{P}_i | B_{f(i)} \rangle. \quad (35)$$

This relation can be introduced in Eq. (27) to obtain a shorter expression for the time evolution of the system state in terms of the product  $\mathbf{P}_g$ ,

$$\begin{aligned}
|X_g\rangle &= \mathbf{P}_g |X_0\rangle + \left(\frac{\eta_g}{\mu_g} - 1\right) \mathbf{P}_g |X_0\rangle, \\
&= \frac{\eta_g}{\mu_g} \mathbf{P}_g |X_0\rangle \\
&= \gamma_g \mathbf{P}_g |X_0\rangle \\
&= \mathbf{P}'_g |X_0\rangle.
\end{aligned} \tag{36}$$

Here,  $\gamma_g \equiv \frac{\eta_g}{\mu_g}$ , is a random number and  $\mathbf{P}'_g \equiv \gamma_g \mathbf{P}_g$  is the original product modulated by  $\gamma_g$ . It is relevant to know the range of values that  $\gamma_g$  could take. To analyze this aspect let's consider the inequality

$$0 \leq \langle X'_g | \mathbf{P}_g | X_0 \rangle < \langle X'_g | \mathbf{P}_g | X_0 \rangle + \langle X'_g | \sum_{i=1}^g \mathbf{P}_i | B_{f(i)} \rangle = \langle X'_g | X_g \rangle < 1 \tag{37}$$

or

$$0 \leq \langle X'_g | \mathbf{P}_g | X_0 \rangle < \langle X'_g | X_g \rangle < 1, \tag{38}$$

i.e.,

$$0 \leq \mu_g < \eta_g < 1. \tag{39}$$

Then,

$$1 < \gamma = \frac{\eta_g}{\mu_g} < \infty. \tag{40}$$

It turns out that  $\gamma$  is an unbounded random variable larger than 1, i.e., applying  $\gamma$  on  $\mathbf{P}_g$  has an amplifying effect.

### Calculating the norm of $|X_g\rangle$

We need to know the behavior of the norm of  $|X_g\rangle$ . To calculate it we have to develop the inner product,

$$\|X_g\| = \langle X_g | X_g \rangle^{1/2} = \langle X_0 | \mathbf{P}'_g^\dagger \mathbf{P}'_g | X_0 \rangle^{1/2}, \tag{41}$$

given that  $\mathbf{P}'_g$  is not a self-adjoint operator. Here  $\mathbf{P}'_g^\dagger$  is the Hermitian conjugate of the operator  $\mathbf{P}'_g$ , i.e., the adjoint matrix in our case. Then, the problem of calculating the norm

translates to the calculation of  $\mathbf{P}'^\dagger \mathbf{P}'_g$ . To evaluate such a product we must write it in terms of the time dependent random matrix  $\mathbf{A}_g$ ,

$$\mathbf{P}'^\dagger \mathbf{P}'_g = \gamma_g^* \mathbf{P}_g^\dagger \gamma_g \mathbf{P}_g = \gamma_g^* \gamma_g \mathbf{P}_g^\dagger \mathbf{P}_g, \quad (42)$$

with

$$\begin{aligned} \mathbf{M}_g &\equiv \mathbf{P}_g^\dagger \mathbf{P}_g = [\mathbf{A}_{g-1} \mathbf{A}_{g-2} \dots \mathbf{A}_1 \mathbf{A}_0]^\dagger \mathbf{A}_{g-1} \mathbf{A}_{g-2} \dots \mathbf{A}_1 \mathbf{A}_0 = \\ &= \mathbf{A}_0^\dagger \mathbf{A}_1^\dagger \dots \mathbf{A}_{g-2}^\dagger \mathbf{A}_{g-1}^\dagger \mathbf{A}_{g-1} \mathbf{A}_{g-2} \dots \mathbf{A}_1 \mathbf{A}_0 = \\ &= \mathbf{A}_0^\dagger [\mathbf{A}_1^\dagger \dots [\mathbf{A}_{g-2}^\dagger [\mathbf{A}_{g-1}^\dagger \mathbf{A}_{g-1}] \mathbf{A}_{g-2}] \dots \mathbf{A}_1] \mathbf{A}_0, \end{aligned} \quad (43)$$

where

$$\mathbf{A}_g^\dagger = \begin{pmatrix} r_g/\beta & 1 \\ -r_g \alpha & 0 \end{pmatrix} \quad (44)$$

### Eigenvalues of $p_1$

In the equation for  $\mathbf{M}_g$ , the core or first inner product is given by

$$p_1 = \mathbf{A}_{g-1}^\dagger \mathbf{A}_{g-1} = \begin{pmatrix} \frac{r_1^2 + \beta^2}{\beta^2} & -\frac{r_1^2}{\beta} \alpha \\ -\frac{r_1^2}{\beta} a & \alpha^2 r_1^2 \end{pmatrix}, \quad (45)$$

where we have use the notation  $r_i \equiv r_{g-i}$ . It should be noted that this matrix has eigenvalues,

$$\lambda_{\pm}^{p_1} = \frac{1}{2\beta^2} \left( (1 + \alpha^2 r_1^2) \beta^2 + r_1^2 \pm \sqrt{(r_1^4 + 2\beta^2 r_1^2 + 2r_1^4 \beta^2 \alpha^2 + \beta^4 - 2\beta^4 \alpha^2 r_1^2 + \beta^4 \alpha^4 r_1^4)} \right) \quad (46)$$

The term inside the square root can be simplified as follows,

$$\begin{aligned} r_1^4 + 2\beta^2 r_1^2 + 2r_1^4 \beta^2 \alpha^2 + \beta^4 - 2\beta^4 \alpha^2 r_1^2 + \beta^4 \alpha^4 r_1^4 &= \\ = (\beta^2 \alpha^2 r_1^2 + \beta^2 + 2\alpha \beta^2 r_1 + r_1^2) (\beta^2 \alpha^2 r_1^2 + \beta^2 - 2\alpha \beta^2 r_1 + r_1^2) &= \\ = ((1 + \alpha^2 r_1^2) \beta^2 + r_1^2)^2 - (2\alpha \beta^2 r_1)^2 &= \\ \equiv \Lambda_1^2 - \Upsilon_1^2, & \end{aligned} \quad (47)$$

where

$$\Lambda_1 \equiv (1 + \beta^2 \alpha^2) r_1^2 + \beta^2, \quad (48)$$

and  $\Upsilon_1 \equiv 2\beta^2 \alpha r_1$ . Therefore, the eigenvalues of the product  $p_1$  can be rewritten as,

$$\lambda_{\pm}^{p_1} = \frac{1}{2\beta^2} \left( \Lambda_1 \pm \sqrt{\Lambda_1^2 - \Upsilon_1^2} \right). \quad (49)$$

### Eigenvalues of $p_2$

Now, let's calculate the second inner product, given by,

$$\begin{aligned}
p_2 &= \mathbf{A}_{g-2}^\dagger p_1 \mathbf{A}_{g-2} = \\
&= \begin{bmatrix} \frac{r_2}{\beta} & 1 \\ -\alpha r_2 & 0 \end{bmatrix} \begin{bmatrix} \frac{r_1^2 + \beta^2}{\beta^2} & -\frac{r_1^2}{\beta} \alpha \\ -\frac{r_1^2}{\beta} \alpha & \alpha^2 r_1^2 \end{bmatrix} \begin{bmatrix} \frac{r_2}{\beta} & -\alpha r_2 \\ 1 & 0 \end{bmatrix} = \\
&= \begin{bmatrix} \frac{r_2^2 r_1^2 + r_2^2 \beta^2 - 2r_2 r_1^2 \alpha \beta^2 + r_1^2 \alpha^2 \beta^4}{\beta^4} & \frac{-r_2 r_1^2 - r_2 \beta^2 + r_1^2 \alpha \beta^2}{\beta^3} \alpha r_2 \\ \frac{-r_2 r_1^2 - r_2 \beta^2 + r_1^2 \alpha \beta^2}{\beta^3} \alpha r_2 & \alpha^2 r_2^2 \frac{r_1^2 + \beta^2}{\beta^2} \end{bmatrix},
\end{aligned} \tag{50}$$

with eigenvalues,

$$\begin{aligned}
\lambda_{\pm}^{p_2} &= \frac{1}{2\beta^4} (r_2^2 r_1^2 + r_2^2 \beta^2 - 2r_2 r_1^2 \alpha \beta^2 + \beta^4 \alpha^2 r_1^2 + \beta^2 \alpha^2 r_2^2 r_1^2 + \beta^4 \alpha^2 r_2^2 \pm \\
&\quad (2r_2^4 r_1^2 \beta^2 + r_2^4 r_1^4 + r_2^4 \beta^4 + 2r_2^4 \beta^6 \alpha^2 + \beta^8 \alpha^4 r_1^4 + \beta^8 \alpha^4 r_2^4 - 4r_2 r_1^4 \alpha^3 \beta^6 \\
&\quad - 4r_2^3 r_1^4 \alpha^3 \beta^4 - 4r_2^3 r_1^2 \alpha^3 \beta^6 + 2\beta^6 \alpha^4 r_1^4 r_2^2 + \beta^4 \alpha^4 r_2^4 r_1^4 + 2\beta^6 \alpha^4 r_2^4 r_1^2 \\
&\quad - 2\beta^8 \alpha^4 r_1^2 r_2^2 - 4r_2^3 r_1^4 \alpha \beta^2 + 6r_2^2 r_1^4 \beta^4 \alpha^2 + 2r_2^4 r_1^4 \beta^2 \alpha^2 + 4r_2^4 r_1^2 \beta^4 \alpha^2 \\
&\quad - 4r_2^3 \beta^4 r_1^2 \alpha + 2r_2^2 \beta^6 \alpha^2 r_1^2)^{1/2}).
\end{aligned} \tag{51}$$

Here, we can define,

$$\Lambda_2 \equiv \begin{bmatrix} (1 + \beta^2 \alpha^2) r_1^2 \\ + (\beta^2 + \beta^4 \alpha^2) \end{bmatrix} r_2^2 + \begin{bmatrix} (-2 \alpha \beta^2) r_1^2 \\ (\beta^4 \alpha^2) r_1^2 \end{bmatrix} r_2 + \begin{bmatrix} (\beta^4 \alpha^2) r_1^2 \\ (\beta^4 \alpha^2) r_1^2 \end{bmatrix}. \tag{52}$$

The term under the square root differs from  $\Lambda_2$  by  $4\alpha^4 r_2^2 r_1^2 \beta^8$

$$(r_2^2 r_1^2 + r_2^2 \beta^2 - 2r_2 r_1^2 \alpha \beta^2 + \beta^4 \alpha^2 r_1^2 + \beta^2 \alpha^2 r_2^2 r_1^2 + \beta^4 \alpha^2 r_2^2)^2 - \tag{53}$$

$$2r_2^4 r_1^2 \beta^2 - r_2^4 r_1^4 - r_2^4 \beta^4 - 2r_2^4 \beta^6 \alpha^2 - \beta^8 \alpha^4 r_1^4 - \beta^8 \alpha^4 r_2^4$$

$$+ 4r_2 r_1^4 \alpha^3 \beta^6 + 4r_2^3 r_1^4 \alpha^3 \beta^4 + 4r_2^3 r_1^2 \alpha^3 \beta^6 - 2\beta^6 \alpha^4 r_1^4 r_2^2$$

$$- \beta^4 \alpha^4 r_2^4 r_1^4 - 2\beta^6 \alpha^4 r_2^4 r_1^2 + 2\beta^8 \alpha^4 r_1^2 r_2^2 + 4r_2^3 r_1^4 \alpha \beta^2$$

$$- 6r_2^2 r_1^4 \beta^4 \alpha^2 - 2r_2^4 r_1^4 \beta^2 \alpha^2 - 4r_2^4 r_1^2 \beta^4 \alpha^2 + 4r_2^3 \beta^4 r_1^2 \alpha - 2r_2^2 \beta^6 \alpha^2 r_1^2$$

$$= 4\alpha^4 r_2^2 r_1^2 \beta^8. \tag{54}$$

Then, we can make use of  $\Upsilon_2 \equiv \sqrt{4\alpha^4 r_2^2 r_1^2 \beta^8} = 2\beta^4 \alpha^2 r_2 r_1$ , to write the eigenvalues of  $p_2$  as  $\lambda_{\pm}^{p_2} = \frac{1}{2\beta^4} (\Lambda_2 \pm \sqrt{\Lambda_2^2 - \Upsilon_2^2})$ .

### Eigenvalues of $p_3$

Similarly, the third inner product, given by,

$$\begin{aligned} p_3 &= \mathbf{A}_{g-3}^\dagger p_2 \mathbf{A}_{g-3} = & (55) \\ &= \mathbf{A}_{g-3} \begin{bmatrix} \frac{r_2^2 r_1^2 + r_2^2 \beta^2 - 2r_2 r_1^2 \alpha \beta^2 + r_1^2 \alpha^2 \beta^4}{\beta^4} & \frac{-r_2 r_1^2 - r_2 \beta^2 + r_1^2 \alpha \beta^2}{\beta^3} \alpha r_2 \\ \frac{-r_2 r_1^2 - r_2 \beta^2 + r_1^2 \alpha \beta^2}{\beta^3} \alpha r_2 & \alpha^2 r_2^2 \frac{r_1^2 + \beta^2}{\beta^2} \end{bmatrix} \mathbf{A}_{g-3}, \end{aligned}$$

has eigenvalues that can be written as  $\lambda_{\pm}^{p_3} = \frac{1}{2\beta^6} \left( \Lambda_3 \pm \sqrt{\Lambda_3^2 - \Upsilon_3^2} \right)$ , where,

$$\begin{aligned} \Lambda_3 \equiv & \left\{ \begin{aligned} & \left[ (1 + \beta^2 \alpha^2) r_1^2 \right] r_2^2 \\ & + \left[ (\beta^2 + \beta^4 \alpha^2) \right] r_2 \end{aligned} \right\} r_3^2 + & (56) \\ & + \left\{ \begin{aligned} & \left[ (-2 \alpha \beta^2 - 2 \beta^4 \alpha^3) r_1^2 \right] r_2 \\ & + \left[ (\beta^4 \alpha^2 + \beta^6 \alpha^4) r_1^2 \right] \end{aligned} \right\} r_3 \\ & + \left\{ \begin{aligned} & \left[ (-2 \alpha \beta^2) r_1^2 \right] r_2^2 \\ & + \left[ (-2 \alpha \beta^4) \right] r_2 \end{aligned} \right\} r_3 \\ & + \left\{ \begin{aligned} & \left[ (2 \alpha^2 \beta^4) r_1^2 \right] r_2 \\ & + \left[ (\beta^4 \alpha^2) r_1^2 \right] r_2^2 \\ & + \left[ (\alpha^2 \beta^6) \right] \end{aligned} \right\} \end{aligned}$$

and  $\Upsilon_3 = 2\beta^6 \alpha^3 r_3 r_2 r_1$ .

### Eigenvalues of $p_4$

Now, the fourth inner product becomes,

$$p_4 = \mathbf{A}_{g-4}^\dagger p_3 \mathbf{A}_{g-4} \quad (57)$$

with eigenvalues  $\lambda_{\pm}^{p_4} = \frac{1}{2\beta^8} \left( \Lambda_4 \pm \sqrt{\Lambda_4^2 - \Upsilon_4^2} \right)$ , where,

$$\Lambda_4 \equiv \left( \begin{array}{c} \left\{ \begin{array}{c} \left[ (1 + \beta^2\alpha^2) r_1^2 \right] r_2^2 \\ + \left[ (\beta^2 + \beta^4\alpha^2) \right] r_2 \end{array} \right\} r_3^2 \\ + \left\{ \begin{array}{c} \left[ (-2\beta^4\alpha^3 - 2\alpha\beta^2) r_1^2 \right] r_2 \\ + \left[ (\beta^6\alpha^4 + \beta^4\alpha^2) r_1^2 \right] \end{array} \right\} r_3 \\ + \left\{ \begin{array}{c} \left[ (-2\beta^4\alpha^3 - 2\alpha\beta^2) r_1^2 \right] r_2^2 \\ + \left[ (-2\beta^6\alpha^3 - 2\alpha\beta^4) \right] r_2 \\ + \left[ (2\beta^6\alpha^4 + 2\beta^4\alpha^2) r_1^2 \right] r_2 \end{array} \right\} r_3 \\ + \left\{ \begin{array}{c} \left[ (\beta^6\alpha^4 + \beta^4\alpha^2) r_1^2 \right] \\ + \left[ (\beta^8\alpha^4 + \alpha^2\beta^6) \right] \end{array} \right\} r_2^2 \end{array} \right) r_4^2 \\ + \left( \begin{array}{c} \left\{ \begin{array}{c} \left[ (-2\alpha\beta^2) r_1^2 \right] r_2^2 \\ + \left[ (-2\alpha\beta^4) \right] r_2 \end{array} \right\} r_3^2 \\ + \left\{ \begin{array}{c} \left[ (4\alpha^2\beta^4) r_1^2 \right] r_2 \\ + \left[ (-2\alpha^3\beta^6) r_1^2 \right] \end{array} \right\} r_3 \\ + \left\{ \begin{array}{c} \left[ (2\beta^4\alpha^2) r_1^2 \right] r_2^2 \\ + \left[ (2\alpha^2\beta^6) \right] r_2 \end{array} \right\} r_3 \\ + \left\{ \begin{array}{c} \left[ (\beta^4\alpha^2) r_1^2 \right] r_2^2 \\ + \left[ (\alpha^2\beta^6) \right] r_2 \end{array} \right\} r_3^2 \\ + \left\{ \begin{array}{c} \left[ (-2\alpha^3\beta^6) r_1^2 \right] r_2 \\ + \left[ (\alpha^4\beta^8) r_1^2 \right] \end{array} \right\} \end{array} \right) r_4 \quad (58)$$

and  $\Upsilon_4 = 2\beta^8\alpha^4 r_4 r_3 r_2 r_1$ .

### Eigenvalues of $p_5$

Here we show  $p_5$ , given by,

$$p_5 = \mathbf{A}_{g-5}^\dagger p_4 \mathbf{A}_{g-5}, \quad (59)$$

with eigenvalues,  $\lambda_{\pm}^{p_5} = \frac{1}{2\beta^{10}} \left( \Lambda_5 \pm \sqrt{\Lambda_5^2 - \Upsilon_5^2} \right)$ , with,

$$\begin{aligned}
\Lambda_5 \equiv & \left[ \left( \left\{ \begin{array}{l} (1 + \beta^2 \alpha^2) r_1^2 \\ + (\beta^2 + \beta^4 \alpha^2) \end{array} \right\} r_2^2 \right) r_3^2 \right. \\
& + \left. \left\{ \begin{array}{l} (-2 \alpha \beta^2 - 2 \beta^4 \alpha^3) r_1^2 \\ + (\beta^4 \alpha^2 + \beta^6 \alpha^4) r_1^2 \end{array} \right\} r_2 \right\} r_4^2 \\
& + \left\{ \begin{array}{l} (-2 \alpha \beta^2 - 2 \beta^4 \alpha^3) r_1^2 \\ + (-2 \beta^6 \alpha^3 - 2 \alpha \beta^4) \end{array} \right\} r_2^2 \left. \right\} r_3 \\
& + \left\{ \begin{array}{l} (2 \beta^6 \alpha^4 + 2 \beta^4 \alpha^2) r_1^2 \\ + (\beta^4 \alpha^2 + \beta^6 \alpha^4) r_1^2 \end{array} \right\} r_2^2 \\
& + \left\{ \begin{array}{l} + (\beta^8 \alpha^4 + \alpha^2 \beta^6) \end{array} \right\} r_2^2 \\
& \left. \left\{ \begin{array}{l} (-2 \alpha \beta^2 - 2 \beta^4 \alpha^3) r_1^2 \\ + (-2 \beta^6 \alpha^3 - 2 \alpha \beta^4) \end{array} \right\} r_2^2 \right\} r_3^2 \left. \right\} r_5^2 \\
& + \left. \left\{ \begin{array}{l} (4 \beta^6 \alpha^4 + 4 \beta^4 \alpha^2) r_1^2 \\ + (-2 \beta^6 \alpha^3 - 2 \beta^8 \alpha^5) r_1^2 \end{array} \right\} r_2 \right\} r_4 \\
& + \left\{ \begin{array}{l} (2 \beta^6 \alpha^4 + 2 \beta^4 \alpha^2) r_1^2 \\ + (2 \beta^8 \alpha^4 + 2 \alpha^2 \beta^6) \end{array} \right\} r_2^2 \left. \right\} r_3 \\
& + \left\{ \begin{array}{l} + (-2 \beta^6 \alpha^3 - 2 \beta^8 \alpha^5) r_1^2 \end{array} \right\} r_2 \left. \right\} r_3^2 \\
& + \left. \left\{ \begin{array}{l} (\beta^4 \alpha^2 + \beta^6 \alpha^4) r_1^2 \\ + (\beta^8 \alpha^4 + \alpha^2 \beta^6) \end{array} \right\} r_2^2 \right\} r_3^2 \\
& + \left. \left\{ \begin{array}{l} + (-2 \beta^6 \alpha^3 - 2 \beta^8 \alpha^5) r_1^2 \\ + (\beta^8 \alpha^4 + \beta^{10} \alpha^6) r_1^2 \end{array} \right\} r_2 \right\} r_3^2 \left. \right\} r_5^2
\end{aligned} \tag{60}$$

$$\begin{aligned}
& + \left[ \left( \begin{array}{c} \left\{ \begin{array}{c} \left[ (-2\alpha\beta^2)r_1^2 \right] r_2^2 \\ + \left[ (-2\alpha\beta^4) \right] r_2 \end{array} \right\} r_3^2 \\ + \left\{ \begin{array}{c} \left[ (4\alpha^2\beta^4)r_1^2 \right] r_2 \\ + \left[ (-2\alpha^3\beta^6)r_1^2 \right] \end{array} \right\} \\ + \left\{ \begin{array}{c} \left[ (4\beta^4\alpha^2)r_1^2 \right] r_2^2 \\ + \left[ (4\alpha^2\beta^6) \right] r_2 \end{array} \right\} r_3 + \left\{ \begin{array}{c} \left[ (-4\alpha^3\beta^6)r_1^2 \right] r_2 \\ \left[ (-2\alpha^3\beta^6)r_1^2 \right] r_2^2 \\ (-2\alpha^3\beta^8) \end{array} \right\} \end{array} \right] r_4^2 \\
& + \left[ \left( \begin{array}{c} \left\{ \begin{array}{c} \left[ (2\beta^4\alpha^2)r_1^2 \right] r_2^2 \\ + \left[ (2\alpha^2\beta^6) \right] r_2 \end{array} \right\} r_3^2 \\ + \left\{ \begin{array}{c} \left[ (-4\alpha^3\beta^6)r_1^2 \right] r_2 \\ + \left[ (2\alpha^4\beta^8)r_1^2 \right] \end{array} \right\} \\ + \left\{ \begin{array}{c} \left[ (-2\alpha^3\beta^6)r_1^2 \right] r_2^2 \\ + \left[ (-2\alpha^3\beta^8) \right] r_2 \\ + \left[ (2\alpha^4\beta^8)r_1^2 \right] r_2 \end{array} \right\} r_3 \end{array} \right] r_4 \\
& + \left[ \left( \begin{array}{c} \left\{ \begin{array}{c} \left[ (\beta^4\alpha^2)r_1^2 \right] r_2^2 \\ + \left[ (\alpha^2\beta^6) \right] r_2 \end{array} \right\} r_3^2 \\ + \left\{ \begin{array}{c} \left[ (-2\alpha^3\beta^6)r_1^2 \right] r_2 \\ + \left[ (\alpha^4\beta^8)r_1^2 \right] \end{array} \right\} \\ + \left\{ \begin{array}{c} \left[ (-2\alpha^3\beta^6)r_1^2 \right] r_2^2 \\ + \left[ (-2\alpha^3\beta^8) \right] r_2 \\ + \left[ (2\alpha^4\beta^8)r_1^2 \right] r_2 \end{array} \right\} r_3 \\ + \left\{ \begin{array}{c} \left[ (\alpha^4\beta^8)r_1^2 \right] r_2^2 \\ + \left[ (\alpha^4\beta^{10}) \right] \end{array} \right\} \end{array} \right] r_4^2
\end{aligned}$$

and  $\Upsilon_5 = 2\beta^{10}\alpha^5 r_5 r_4 r_3 r_2 r_1$ .

## Nested structures

The analysis of the previous section demonstrate that the eigenvalues of the products,  $p_1, p_2, \dots, p_N$ , can be expressed shortly as,

$$\lambda_{\pm}^{p_g} = \frac{1}{2\beta^{2g}} \left( \Lambda_g \pm \sqrt{\Lambda_g^2 - \Upsilon_g^2} \right), \quad (61)$$

where terms  $\Lambda_g$  and  $\Upsilon_g$  are polynomials in the noise terms, i.e., random polynomials. In particular,  $\Upsilon_g$ , can be easily written in compact form as,

$$\Upsilon_g = 2\beta^{2g} \alpha^g \prod_{i=1}^g r_i. \quad (62)$$

Instead, a closed form for  $\Lambda_g$  is more harder to find. It is so because  $\Lambda_g$  follows the complex nested structure seen in the previous sections that is unveiled here. Note that  $\Lambda_g$  is a polynomial in  $r_g$  of order two whose coefficients are polynomials of order two in  $r_{g-1}$ , whose coefficients are polynomials of order two in  $r_{g-2}$ , and so on. Let's say that  $C : C(r_{g-1}, \dots, r_1)$  is a function that depends on the noise terms  $r_{g-1}, \dots, r_1$ . Let's also say that this function is a coefficient of a noise term of order  $i$ , i.e., that a second order polynomial has terms  $C_i(r_{g-1}, \dots, r_1)r^i$ . Now, depending on what  $\Lambda_g$  are we dealing with we shall distinguish each of these functional coefficients. Consequently, it is convenient indexing also the  $C$ 's to make such a distinction, so to have polynomial terms  $C_{i,g}(r_{g-1}, \dots, r_1)r_g^i$ . Here, we have also indexed  $r_g$  because that noise's value is exactly the one at step  $g$ . Accordingly,  $\Lambda_g$  can be conveyed to,

$$\begin{aligned} \Lambda_g &= \sum_{i=0}^2 C_{g,i}(r_{g-1}, \dots, r_1)r_g^i \\ &= \sum_{i=0}^2 C_{g,i,1}r_g^i, \end{aligned} \quad (63)$$

with  $C_{g,i}(r_{g-1}, \dots, r_1) |_{g=1} \equiv C_{1,i} : \text{constant}$ . Note we have not indexed the nested levels. The main reason is that there is no need for that: we can reproduce the full structure as follows. In general, if we know  $\Lambda_1$  and  $\Lambda_2$ , we can obtain  $\Lambda_g$  given that, in the generation  $g-1$  the term,

$$\{C_2r_i^2 + C_1r_i + C_0\}r_{i+1}^k \quad \text{with} \quad k = 0, 1, 2, \quad (64)$$

generates the polynomial,

$$\left\{ \begin{array}{l} [C_2 r_i^2 + C_1 \chi_1 r_i + \beta^2 C_2] r_{i+1}^2 \\ + [-k\alpha\beta^2 C_2 r_i^2 + C_1 \chi_2 r_i + C_1 \chi_3] r_{i+1} \\ + [\beta^2 \alpha^2 C_0 r_i^2 + C_1 \chi_4 r_i + C_1 \chi_5] \end{array} \right\} r_{i+2}^k \quad (65)$$

in the next generation  $g$ . Note that there is no need to determine the unknowns,  $\chi_1, \chi_2, \dots, \chi_5$ , because in the present situation  $C_1 = 0$ .

### Generating nested structures: an example

The preceding procedure is better illustrated with an example: let's find  $\Lambda_3$  from  $\Lambda_2$ , which is given by eq. (52). The coefficient for the quadratic term is,  $[(1 + \alpha^2\beta^2)r_1^2 + \beta^2(1 + \alpha^2\beta^2)]$ , therefore,  $C_2 = 1 + \alpha^2\beta^2$ ,  $C_1 = 0$  and  $C_0 = \beta^2(1 + \alpha^2\beta^2)$ ; and the quadratic term in  $r_3$  is generated as,

$$\left\{ \begin{array}{l} [(1 + \alpha^2\beta^2)r_1^2 + \beta^2(1 + \alpha^2\beta^2)] r_2^2 \\ + [-2\alpha\beta^2(1 + \alpha^2\beta^2)r_1^2] r_2 \\ + [\beta^4\alpha^2(1 + \alpha^2\beta^2)r_1^2] \end{array} \right\} r_3^2. \quad (66)$$

Now, the lineal term in  $\Lambda_2$  is  $-2\alpha\beta^2 r_1^2$ , therefore in this case,  $C_2 = -2\alpha\beta^2$  and  $C_1 = C_0 = 0$ . Then the linear term in  $r_3$  is,

$$\left\{ \begin{array}{l} [(-2\alpha\beta^2)r_1^2 + (-2\alpha\beta^4)] r_2^2 \\ + [2\alpha^2\beta^4 r_1^2] r_2 \end{array} \right\} r_3. \quad (67)$$

Finally, the coefficient of the independent term in  $\Lambda_2$  is  $(\alpha^2\beta^4)r_1^2$ . Then  $C_2 = \alpha^2\beta^4$  and  $C_1 = C_0 = 0$ , so we obtain,

$$\left\{ [(\alpha^2\beta^4)r_1^2 + \alpha^2\beta^6)] r_2^2 \right\} r_3^0. \quad (68)$$

Adding Eq. (66), (67) and (68) results in the term  $\Lambda_3$ .

### Determining the leading term in $\lambda$

From the previous sections it is clear that the eigenvalues of  $\mathbf{M}_g$  are given by

$$\lambda_{\pm}^{p_g} = \frac{1}{2\beta^{2g}} \left( \Lambda_g \pm \sqrt{\Lambda_g^2 - \Upsilon_g^2} \right). \quad (69)$$

However, Eq. (62) indicates that the term  $\Upsilon_g$  grows as a power of the noise term, i.e.,  $\Upsilon_g \sim r^g$ . Meanwhile, equations (48), (52), (56), (58) and (60) tell us that the  $\Lambda_g$ 's grow as a sum of powers of noise terms, i.e.,

$$\begin{aligned}\Lambda_1 &\sim r^2 \\ \Lambda_2 &\sim r^4 + r^3 + r^2 \\ \Lambda_3 &\sim r^6 + r^5 + r^4 + r^3 + r^2 \\ \Lambda_4 &\sim r^8 + r^7 + r^6 + r^5 + r^4 \\ \Lambda_5 &\sim r^{10} + \dots + r^4.\end{aligned}\tag{70}$$

So,  $\Lambda_g > \Upsilon_g$  and  $\Lambda_g$  will predominate for  $g$  sufficiently large, i.e.,  $\frac{\Upsilon_g}{\Lambda_g} \rightarrow 0$ , thus Eq. (61) yields,

$$\begin{aligned}\lambda_+^{p_g} &\sim \Lambda_g + O\left(\frac{\Upsilon_g}{\Lambda_g}\right) \\ \lambda_-^{p_g} &\sim 0 + O\left(\frac{\Upsilon_g}{\Lambda_g}\right)\end{aligned}\tag{71}$$

Let's unpack Eq. (41) to determine the implications of this approximation on the norm  $\|X_g\|$ ,

$$\begin{aligned}\|X_g\| &= \gamma_g^* \gamma_g \langle X_0 | \mathbf{M}_g | X_0 \rangle^{1/2} \\ &= \gamma_g \left[ (x_0 y_0) \begin{pmatrix} \lambda_+ & 0 \\ 0 & \lambda_- \end{pmatrix} \begin{pmatrix} x_0 \\ y_0 \end{pmatrix} \right]^{\frac{1}{2}}.\end{aligned}\tag{72}$$

Combining this equation with the Eqs. (71) we find that  $\Lambda_g$  leads the behavior of the norm,

$$\|X_g\| \sim \frac{\gamma_g}{\beta^g} \sqrt{\Lambda_g} x_0.\tag{73}$$

---

\* juluisca@gmail.com

- [1] L. F. Richardson, Proceedings of the Royal Society of London Series A **110**, 709 (1926).
- [2] A. N. Kolmogorov, Soviet Physics Uspekhi **10**, 734 (1968).
- [3] G. L. Eyink and K. R. Sreenivasan, Rev. Mod. Phys. **78**, 87 (2006).
- [4] R. Ecke, Los Alamos Sci. **29**, 124 (2005).
- [5] A. M. Obukhov, Dok. Akad. Nauk. SSSR **32**, 22 (1941).

- [6] L. Onsager, Phys. Rev. **68**, 286 (1945).
- [7] W. Heisenberg, Zeitschrift für Physik **124**, 628 (1948).
- [8] C. F. v. Weizsäcker, Zeitschrift für Physik **124**, 614 (1948).
- [9] L. Biferale, M. Blank, and U. Frisch, Journal of Statistical Physics **75**, 781 (1994).
- [10] U. Frisch, *Turbulence: The Legacy of A. N. Kolmogorov* (Cambridge University Press, 1995).
- [11] K. R. Sreenivasan, The Physics of Fluids **27**, 1048 (1984).
- [12] A. La Porta, G. A. Voth, A. M. Crawford, J. Alexander, and E. Bodenschatz, Nature **409**, 1017 (2001).
- [13] P. W. Hammer, N. Platt, S. M. Hammel, J. F. Heagy, and B. D. Lee, Phys. Rev. Lett. **73**, 1095 (1994).
- [14] F. Rödelsperger, A. Čenys, and H. Benner, Phys. Rev. Lett. **75**, 2594 (1995).
- [15] C.-S. Poon and C. K. Merrill, Nature **389**, 492 (1997).
- [16] D. L. Feng, C. X. Yu, J. L. Xie, and W. X. Ding, Phys. Rev. E **58**, 3678 (1998).
- [17] A. Krawiecki, J. A. Holyst, and D. Helbing, Phys. Rev. Lett. **89**, 158701 (2002).
- [18] J. L. Cabrera and J. G. Milton, Phys. Rev. Lett. **89**, 158702 (2002).
- [19] A. Veltri and V. Carbone, Phys. Rev. Lett. **92**, 143901 (2004).
- [20] E. A. Spiegel, “Chaos and intermittency in the solar cycle,” (Springer New York, New York, NY, 2009) pp. 25–51.
- [21] F. Freyer, K. Aquino, P. A. Robinson, P. Ritter, and M. Breakspear, The Journal of Neuroscience **29**, 8512 (2009).
- [22] V. Trifonov, L. Pasqualucci, R. Dalla-Favera, and R. Rabadan, Scientific Reports **1**, 191 (2011).
- [23] L. Onsager, Il Nuovo Cimento (1943-1954) **6**, 279 (1949).
- [24] S. G. Saddoughi and S. V. Veeravalli, J. Fluid Mechanics **268**, 333 (1994).
- [25] J. P. Eckmann, Rev. Mod. Phys. **53**, 643 (1981).
- [26] T. Bohr, M. H. Jensen, G. Paladin, and A. Vulpiani, *Dynamical Systems Approach to Turbulence* (Cambridge University Press, Cambridge, 1998).
- [27] J. M. McDonough, Phys. Rev. E **79**, 065302 (2009).
- [28] J. L. Cabrera and J. G. Milton, Chaos: An Interdisciplinary Journal of Nonlinear Science **14**, 691 (2004).
- [29] R. N. Mantegna and H. E. Stanley, Nature **376**, 46 (1995).

- [30] J. Maynard Smith, *Mathematical Ideas in Biology* (Cambridge University Press, 1968).
- [31] D. G. Aronson, M. A. Chory, G. R. Hall, and R. P. McGehee, Communications in Mathematical Physics **83**, 303 (1982).
- [32] J. R. Pounder and T. D. Rogers, Bulletin of Mathematical Biology **42**, 551 (1980).
- [33] Y. Morimoto, Physics Letters A **134**, 179 (1988).
- [34] J. L. Cabrera and F. J. de la Rubia, Physics Letters A **197**, 19 (1995).
- [35] J. L. Cabrera and F. J. de la Rubia, International Journal of Bifurcation and Chaos **06**, 1683 (1996).
- [36] J. L. Cabrera and F. J. d. l. Rubia, Europhys. Lett. **39**, 123 (1997).
- [37] J. L. Cabrera, J. Gorroñogoitia, and F. J. de la Rubia, Phys. Rev. Lett. **82**, 2816 (1999).
- [38] H. Yang and E. Ding, Phys. Rev. E **50**, R3295 (1994).

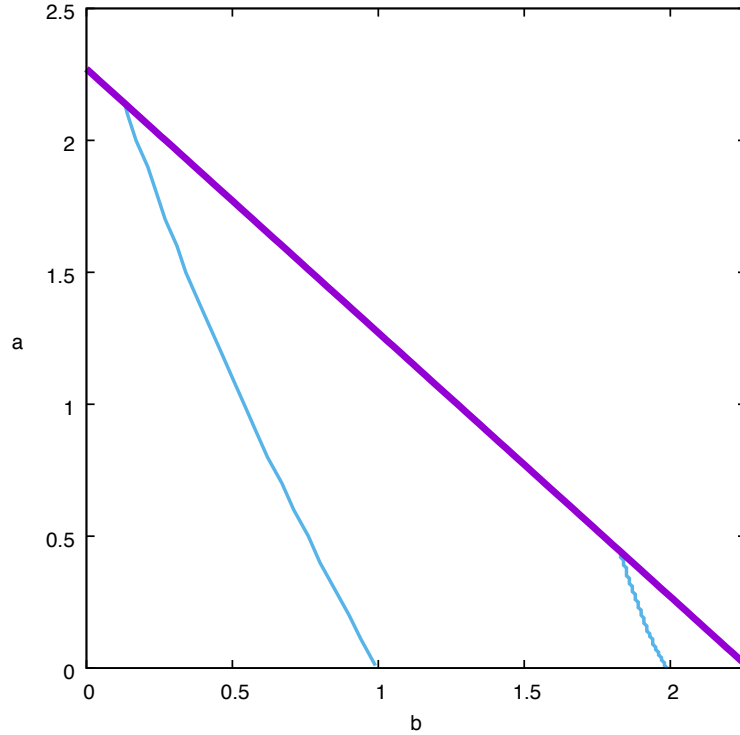


FIG. 6. Blue: stability boundaries for the appearance of on-off intermittency in the Eq. (7) on the  $(a, b)$  plane. Left boundary is for the destabilization of the origin while right one is for the destabilization of  $1 - \frac{1}{\langle r_g \rangle}$ . The boundaries were calculated using the maximum Lyapunov exponent as in [38]. For parameter values close but not on the boundaries the sustained character of the intermittency will be lost in the long run, but intermittent behavior is still present during long time intervals. Magenta: finite solutions  $(a + b)$ -parameter region for Eq. (7) [33–35].